3rd and Final reporting for ActILab

This reports covers the Milestones and Deliverable for the 3rd and last reporting period of ENSAR from 1st Sept 2013 to 31st Dec 2014. Four Milestones were anticipated in the previous period, that is MS85 *Synthesis of actinide targets by sol-gel method - 'chimie douce'*, MS86 *Synthesis of nanostructured actinide targets*, MS87 *Characterization of structures* and MS90 *Analysis of online tests of new actinide targets*.
In this reporting period, the remaining three Milestones and four Deliverable were achieved and are now reported in the subsequent part for each of the four Tasks of ActILab.

TASK #1 (COORDINATION C. LAU – IPNO): SYNTHESIS OF NEW ACTINIDE TARGETS

D8.1 Novel synthesis of actinide targets

Various uranium carbide target materials have been synthesized following new synthetical routes. This includes different uranium precursors and graphite charges. The list of the new uranium carbide meterials are displayed in table 1, and their main characteristics are displayed in table 2.

Sample	Uranium	Carbon	ratio C/U	Milling of uranium powder	Carburization
OXA	IPNO oxalate	Graphite	3	No	16h at 1770°C
COMP30	IPNO oxalate	Graphite +30 wt % of microfibres	3	No	16h at 1770°C
PARRNe 371	natural UO_2 depleted 0.3% - ref. MN371	Graphite	6	Mixer miller PM100 RETSCH	16h at 1770°C
PARRNe 894	natural UO_2 depleted 0.25% - ref. MN894	Graphite	6	Mixer	16h at 1770°C
PARRNe 894 BP	natural UO_2 depleted 0.25% - ref. MN894	Graphite	6	Planetary miller PM200 RETSCH	16h at 1770°C
CNT	Westinghouse UO_2	Carbone nanotubes	6	No	20 min at 1600°C

Table 1: List of the different UCx materias synthesized during ActILab.

Physicochemical characterizations were systematically performed to describe the structure and microstructure of the carburized pellets (Table 2).

Sample	Phase(1) and their relative proportion (wt %)	Effective density(2) ($g.cm^{-3}$, $\pm$ 0.2)	Open porosity(2) (%)	Closed porosity(2) (%)
OXA	UC / UC_2 and 70.5 / 29.5	12.2	26	7
COMP30	UC / UC_2 and 8.6 / 91.4	10.1	48	13
PARRNe 371	UC / UC_2 and 10.6 / 89.4	8.3	46	4

PARRNe 894	UC / UC_2 and 10.9 / 89.1	8.0	56	8
PARRNe 894 BP	UC / UC_2 and 5.8 / 94.2	8.2	44	6
CNT	UC / UC_2 and 14.7 / 85.3	8.5	77	5

Table 2 : Physicochemical characterizations obtained by X-Ray Diffraction XRD(1) and He pycnometry (2).

A nanostructured uranium carbide target load was produced and tested with a proton beam from PSB at CERN-ISOLDE. The small sized UO_2 powder precursor and the produced pellets are shown on Figure 1.

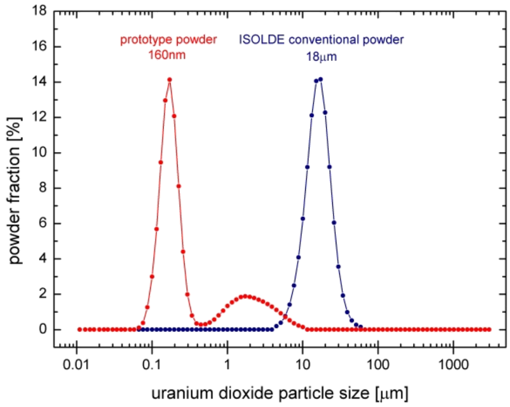

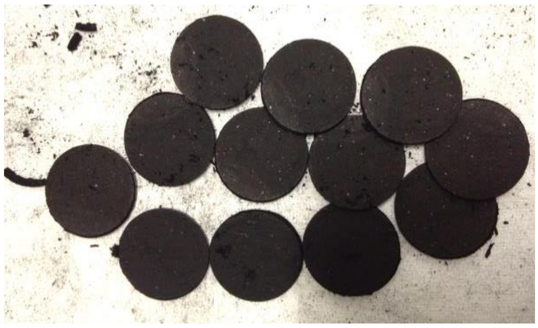

Figure 1 : reduced grain size distribution of the nano UO2 versus the standard powder used, left. A set of pressed pellets used for a target nanoUCx load before online tests (14mm diameter), right.

References:

[1] Hy, B. et al. "An off-line method to characterize the fission product release from uranium carbide-target prototypes developed for SPIRAL2 project." *Nuclear Instruments and Methods in Physics Research Section B: Beam Interactions with Materials and Atoms* 288 (2012): 34-41.

[2] Fernandes, S.et al., *"Microstructure evolution of nanostructured and submicrometric porous refractory ceramics induced by a continuous high-energy proton beam"; Journal of Nuclear Materials 416(1-2) (2011) 99-110*

[3] Ramos, J. P. et al., *"Intense Ar31-35 beams produced with a nanostructured CaO target at ISOLDE",* " *Nuclear Instruments and Methods in Physics Research Section B: Beam Interactions with Materials and Atoms* 320 (2014) 83-88

TASK #2 (COORDINATION A. ANDRIGHETTO – INFN): CHARACTERIZATION OF NEW ACTINIDE TARGETS

MS88 Characterization of thermal properties

Emessivity and thermal conductivity was measured with a new device and the feasibility tested with uranium carbide as seen on Figure 2.

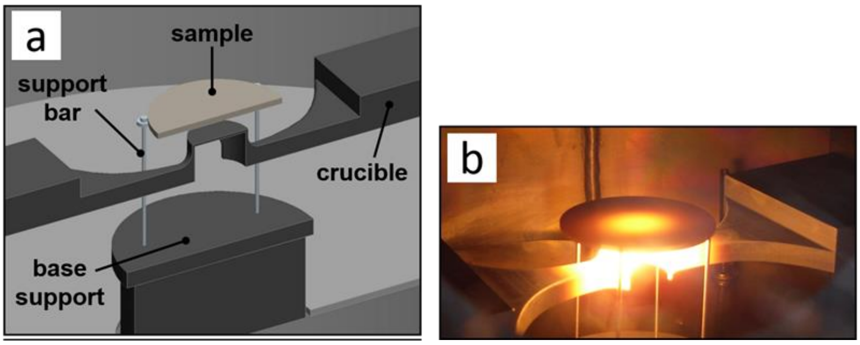

Figure2: a) CAD view of the thermal conductivity estimation setup, b) sample heated by irradiation by the crucible, with the creation of a temperature gradient.

The measured thermal gradient is used to determine the heat conductivity by a analytical fit, as seen on Figure 3. The emissivity is also measured by optical pyrometry.

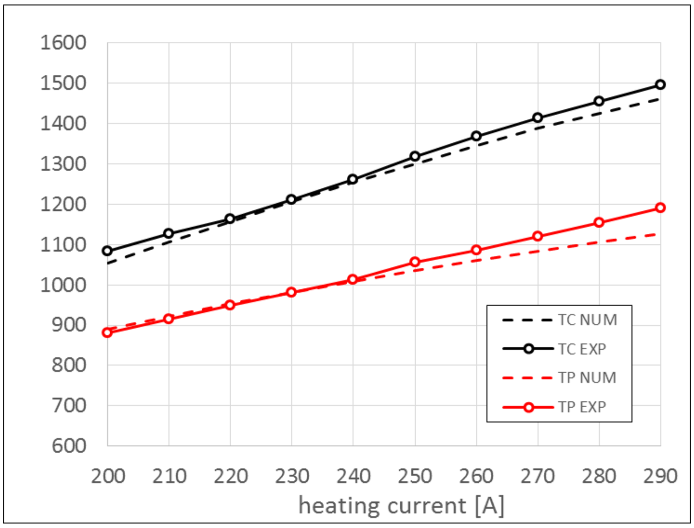

Figure 3. Experimental and numerical temperatures on center and periphery of a UC_X disc.

References:
[4] M. Manzolaro, S. Corradetti, A. Andrighetto, L. Ferrari, A steady-state high temperature method for measuring thermal conductivity of refractory materials, Rev. Sci. Instrum. 84 (2013) 054902.

D8.2 Characterization of new actinide targets

Both thermal and structural properties were determined for a set of uranium carbide prospective materials.

The emissivity of the different materials is shown on Figure 4.

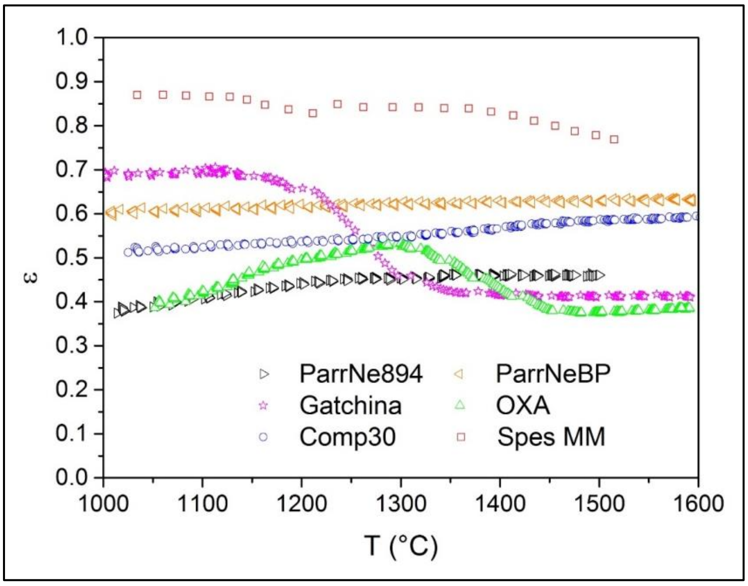

Figure 4. Thermal emissivity of different types of uranium carbide; Gatchina is a dense UC pellet, 12.9 g/cm^3, so called "high density UC". The SPES MM sample is a large disk of UO_2 powder reacted with graphite powder of 29mm diameter, 3.9 g/cm^3 density.

Both the crystalline phase, microstructures, and porosity were determined as shown on figure 5, 6 and 7.

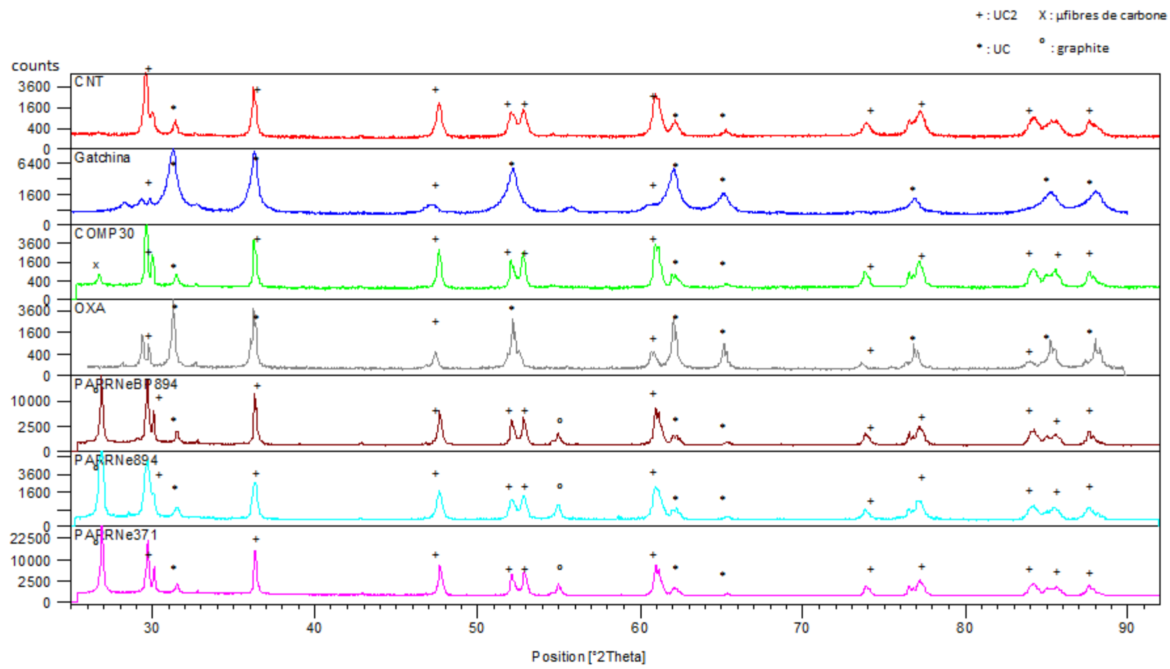

Figure5. XRD patterns of different samples, highlighting the presence of UC, UC_2, graphite and carbon microfibres.

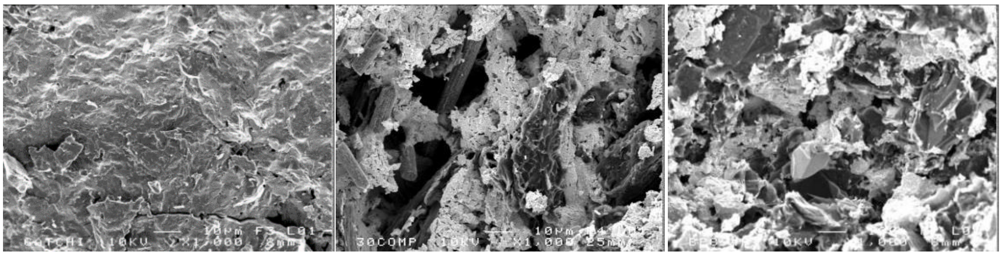

Figure 6. SEM images. From left to right: compact structure of high-density UC, open structure containing UC_2 grains and carbon fibers, open structure containing UC_2 grains and graphite residual clusters (black blocks).

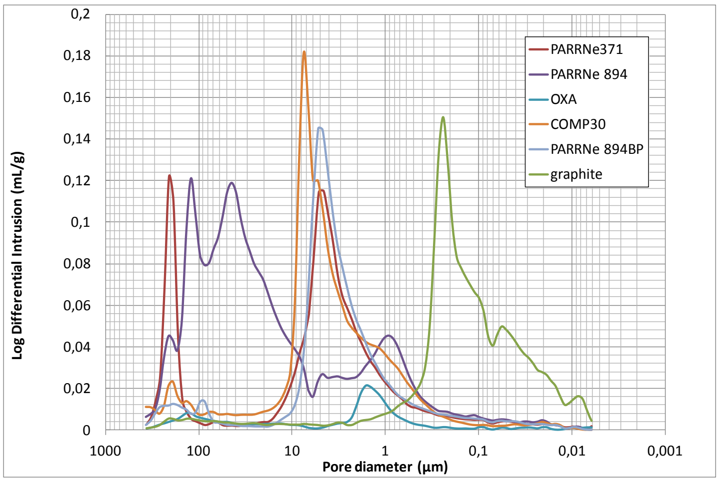

Figure 7. Pore size distribution of different samples using mercury porosimetry.

TASK #3 (COORDINATION M. MARTIN – PSI): ACTINIDE TARGETS PROPERTIES AFTER IRRADIATION

D8.3 Characterization of irradiated materials in hot cell

An irradiated target from Isolde was shipped to PSI and the unit was disassembled, the target container opened and three samples were extracted for further analysis as seen on Figure 8.

Figure 8: uranium carbide target extracted from the middle of the target container in the hot cell

The material was analyzed by Electron Probe MicroAnalyser (EPMA) and Scanning Electron Microscopy. It was compared with a reference unirradiated sample. No significant differences could be observed between these different samples as seen on figure 9.

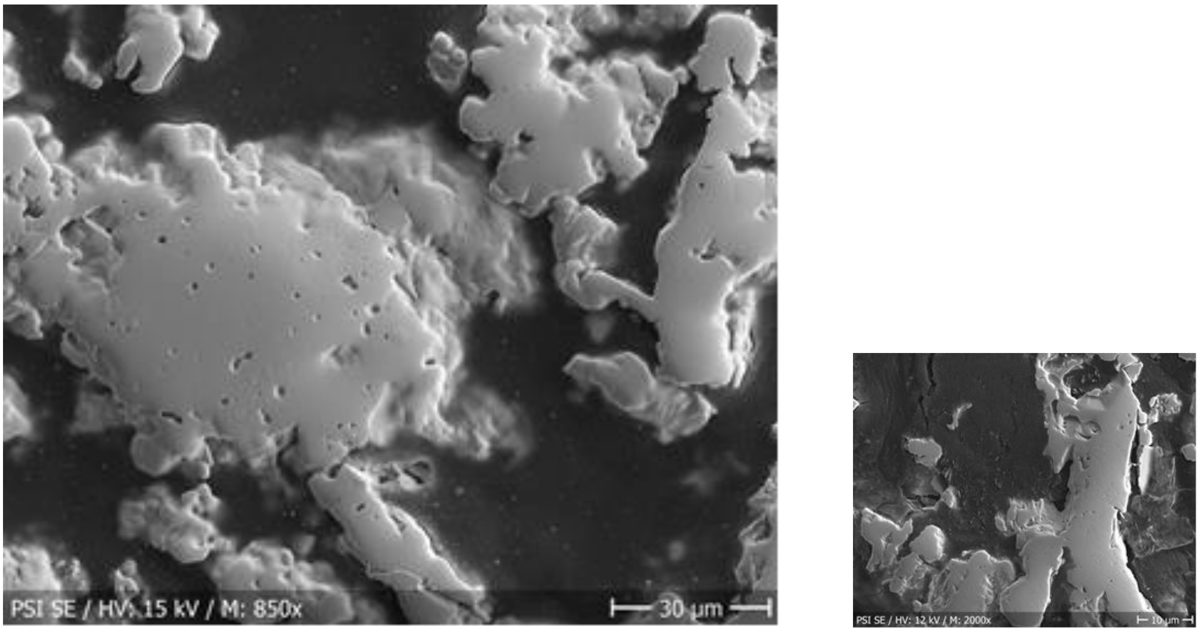

Figure 9: standard UCx target material before irradiation, left; UCx target after irradiation, right. The size of the pictures have been adapted to represent the same scale.

Futher to these investigations, the target materials have been prepared with a FIB milling and analyzed with at the Swiss Light Source. There phase competition between UC and α-UC2at the grain level could be identified for the first time, as shown on Fig.10.

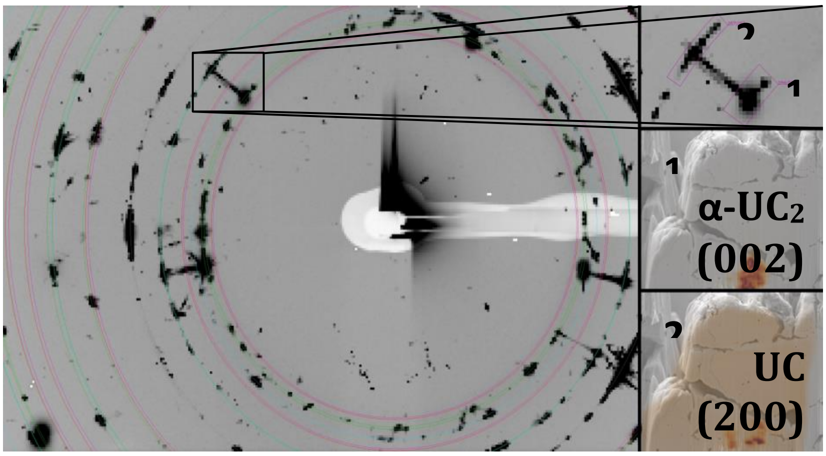

Figure 10: XRD pattern of the investigated UCx; A zoom shows an inelastix scattering path between two coexisting UC and UC2 submicron phase domains.

TASK #4 (COORDINATION H. FRANBERG-DELAHAYE – GANIL): ONLINE TESTS OF ACTINIDE TARGETS

MS91 Effect of beam time structure on online tests

The impact of the time structure of the proton pulse at Isolde, CERN, has been investigated on a standard UCx target and a newly developed nanostructured target. The yield of a representative isotope, 30Na, has been followed in both cases. We can see that a decrease by two orders of magnitude is observed on the standard UCx, while no or very little drop is seen with the nanoUCx target developed within ActILab, Figure 11.

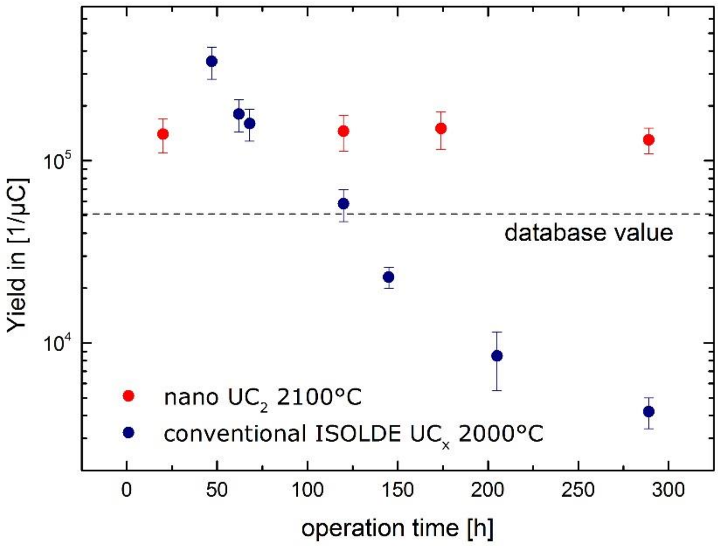

Figure 11: Comparison of impact of the proton beam pulsed tile structure on the evolution of the yield for 30Na at Isolde.

For the case of many exotic radioisotopes the beam intensity reduces over time more or less drastically, making the planning of an experimental campaign challenging. Fig. 2 shows this ageing effect as observed on conventional UC_x target materials (blue points) for short-lived ($T_{1/2}$ = 48 ms) in comparison to the novel ActILab nano UC_2 (red points). Over the time of a typical ISOLDE target life cycle (5-15 days) a drastic drop of isotope rates of two orders of magnitude has been observed for ^{30}Na from several conventional UC_x target units at ISOLDE. Assuming that losses are caused entirely by the growth of uranium carbide particles (sintering) and consequent decay of ^{30}Na during diffusion, a simple diffusion model (R. Kirchner, NIM B, **B70**, 186-199 (1992)) can be employed to relate every observed yield to a certain particle size. Since the temperature dependant diffusion constants *D(T)* of Na in UC and UC_2 is not known an assumption has to be made that can describe the initial crystallite size of both, the non-irradiated UC_x (see MS87) and the irradiated UC_x (see MS89) observed in synchrotron-based micro X-ray diffraction studies. The resulting particle size evolution is shown in Fig. 12. Two domains of particle growth rate can be found in this way, indicating two competing mechanisms of sintering

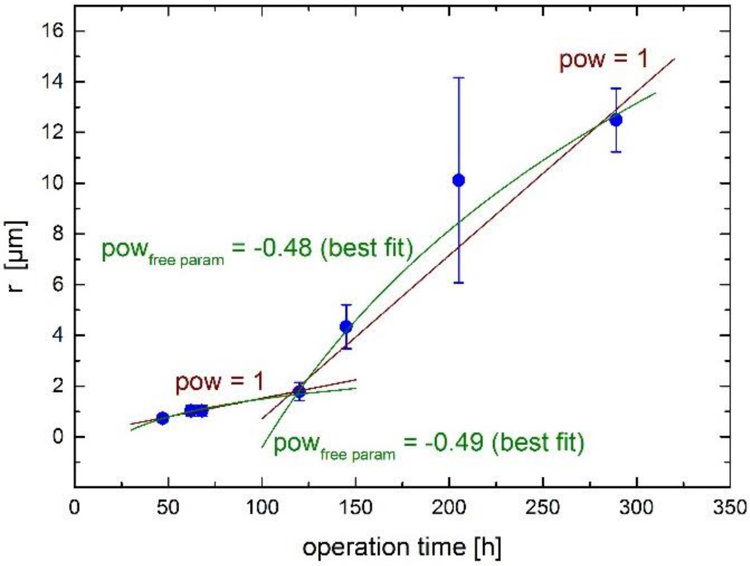

Figure 12: UC_x particle size evolution assuming that losses of ^{30}Na occur uniquely due to nuclear decay during diffusion and assuming a diffusion constant $D=6\cdot10^{-11}$ $cm^{-2}s$.
In the beginning sintering is kinematically hindered and accelerates once carbon diffusion causes a microscopically homogeneous carbon content.

D8.4 Isotope release properties and modelling

The isotope yields have been compared between a standard UCx target and a nanostructured target operated at Isolde, Figure 13. The different release characteristics can be seen on the Figure. For many of the isotopes investigated, increased and steady yields have been observed, Figure 14

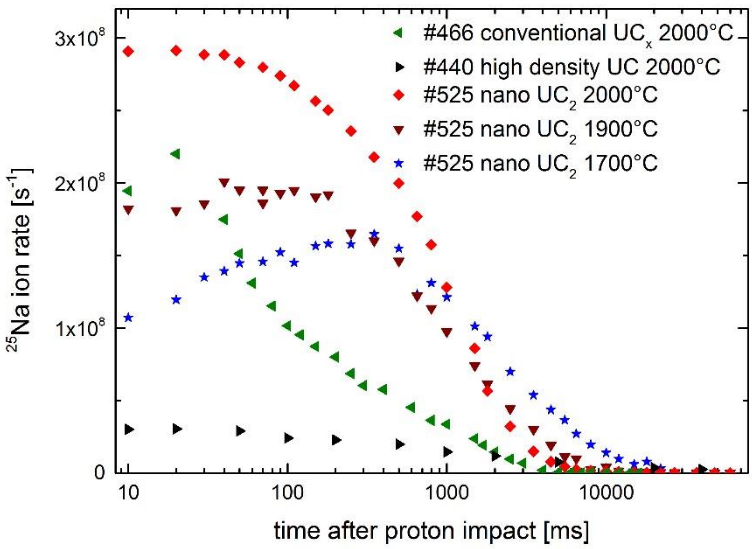

Figure 13: The release structure of ^{25}Na ions after a proton pulse at t=0 for different target materials and temperatures. The different release components are clearly visible that occur as a function of time.

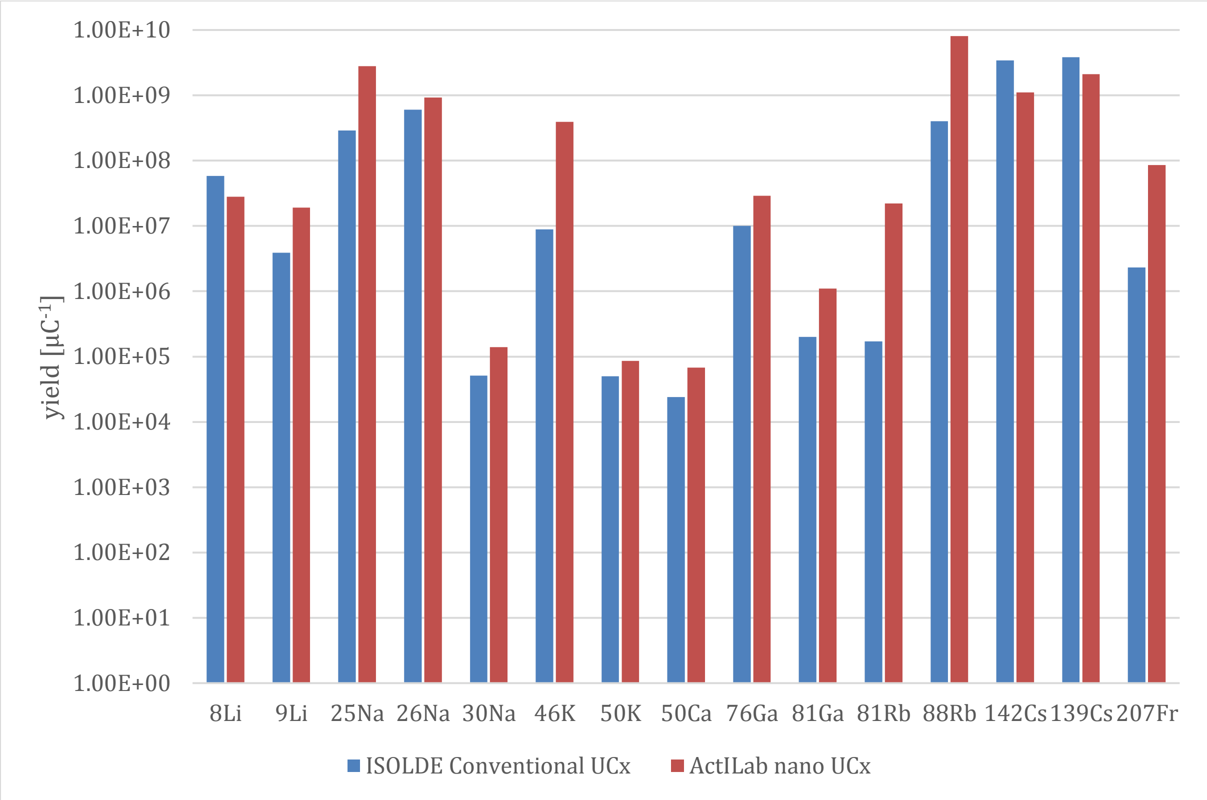

Figure 14. Preliminary results of the ActILab nano-structured UCx (#525UC-Re) in comparison to conventional ISOLDE UCx targets. The references are mostly taken from the ISOLDE yield database, or in the case of 26Na from a measurement on target #410 UC-W, and for 88Rb from #301UC-Ta

Conclusion

The institutes involved in ActILab have used the allocated material resources and manpower as initially foreseen. All Milestones and Deliverables have been achieved, with significant findings and impact for the present and next-generation ISOL facilities.